

Advances on Material Science and Manufacturing Technologies

Edited by
Qingzhou Xu



TRANS TECH PUBLICATIONS

Advances on Material Science and Manufacturing Technologies

Edited by
Qingzhou Xu

Advances on MaterialScience and Manufacturing Technologies

Selected, peer reviewed papers from the
International Conference on
Materials Science and Manufacturing
(ICMSM2012),
December 14-16, 2012, Zhangjia Jie, China

Edited by

Qingzhou Xu



Copyright © 2013 Trans Tech Publications Ltd, Switzerland

All rights reserved. No part of the contents of this publication may be reproduced or transmitted in any form or by any means without the written permission of the publisher.

Trans Tech Publications Ltd
Kreuzstrasse 10
CH-8635 Dürnten-Zürich
Switzerland
<http://www.ttp.net>

Volume 621 of
Advanced Materials Research
ISSN print 1022-6680
ISSN cd 1022-6680
ISSN web 1662-8985

Full text available online at <http://www.scientific.net>

Distributed worldwide by

Trans Tech Publications Ltd
Kreuzstrasse 10
CH-8635 Dürnten-Zürich
Switzerland

Fax: +41 (44) 922 10 33
e-mail: sales@ttp.net

and in the Americas by

Trans Tech Publications Inc.
PO Box 699, May Street
Enfield, NH 03748
USA

Phone: +1 (603) 632-7377
Fax: +1 (603) 632-5611
e-mail: sales-usa@ttp.net

Preface

The International Conference on Materials Science and Manufacturing (ICMSM2012) provided a forum for academic scientists, leading engineers, industry researchers and scholar students to exchange and share their experiences and research results. ICMSM2012 aims to cover the recent advancement and trends in the area of new materials, advanced materials, advanced manufacturing technologies, and manufacturing systems and automation to facilitate knowledge sharing and networking interactions on emerging trends and new challenges.

This book tends to collect the latest research results and applications on material science and manufacturing system and technology. It includes a selection of 77 papers from 212 papers submitted to the conference from universities and industries all over the world. All of accepted papers were subjected to strict peer-reviewing by 2-4 expert referees. The papers have been selected for this volume because of quality and the relevance to the conference.

The editor hopes this book will provide readers a broad overview of the latest advances on material science and manufacturing technologies. The editor also believes this book would be a good reference for academic researchers and industrial professionals in the fields of material science and manufacturing technologies.

ICMSM2012 would like to express our sincere appreciations to all authors for their contributions to this book. We would like to extend our thanks to all the referees for their constructive comments on all papers; especially, we would like to thank to organizing committee for their hard working. Finally, we would like to thank the Trans Tech Publications for producing this volume.

Dr. Qingzhou Xu

Morehead State University

Morehead, Kentucky, USA 40351

2012 International Conference on Materials Science and Manufacturing (ICMSM2012)

Organizing Committee

General Chairs:

Dr. Joe Ashby, Indiana State University

Local committee chair

Dr. Li Tan, Huazhong University of Science and Technology

Technical program committee

Prof. Jinshu Wang, Beijing University of Technology, China

Prof. Libin, Central South University, China

Prof. Jianping Niu, Shenyang University, China

Prof. Qiucheng Wang, Zhejiang University of Technology, China

Dr. Li Tan, Huazhong University of Science and Technology, China

Dr. Qian Lv, Western Digital Inc., USA

Dr. Xiaolong Li, Indiana State University, USA

Dr. Gabriel Alungbe, University of Cincinnati, USA

Dr. Wei Li, Beihang University, China

Dr. Mingsi Su, Lanzhou University, China

Table of Contents

Preface and Organizing Committee

Chapter 1: New Materials and Advanced Materials

Investigation on Nano-Sized ZnO Powder Doped with Al³⁺ Prepared by Sol-Gel Method Y. Xiong, J. Zheng, S.L. Li, X.J. Liu and L. Liang	3
Mechanical Properties of Recycled Butyl Rubber/Virgin Butyl Rubber Composite L. Li and J.K. Kim	8
Synthesis and Characterization of Acrylamide Based Benzoxazine E. Bakangura, Z.Y. Luo, G.K. Wang, Y. Bin, Y.P. Yue and X.D. Lin	11
Mineralogical Study of Huashan Granite-Type Uranium Ore Deposit in Northeast of Guangxi Z.Q. Kang, Z.H. Feng, Y.G. Huang, H.Y. Chen, W. Fu and J.F. Liao	17
Effects of Individual Layer Thickness on the Structure and Electrical Properties of Sol-Gel-Derived Ba_{0.8}Sr_{0.2}TiO₃ Thin Films W. Rao, D.G. Li and H.C. Yan	23
Research Progress of Application of Porous Polymer in Energy Storage Z. Fang and Y. Yang	27
Preparation and Properties of Graphene/Polyamide 6 Composites by Melt Compounding P.P. Zhang, K.Y. Zhu, L.Q. Su and R. Xiao	31
The Effects of B₂O₃ Addition and Sintering Temperature on the Electrical Properties of SnO₂ Based Varistors J.W. Fan, D. Liu, X.L. Zhang, H.J. Zhao, Z.G. Zhang and Y. Zheng	35
A Research of the Spongy Foams from Interpenetrating Polymer Network of Polyurethane/Epoxy Resin H.J. Huang, W. Kang, G.S. Wan and J. Lei	39
Preparation of Flame Retardant Polyamide 6 Fibers with Melamine Cyanurate and Bicyclic Phosphates via Melt Spinning Y.Z. Lin, K. Sha, H.Y. Xu, Y. Tang and R. Xiao	44
Study on the Properties of Poplar Micro/Nanofibril and its Composites Y.P. Liu, J.T. Zhang, X.Y. Luo and Y.Y. Yao	48
A Study on Modification Technology of Poplar through Impregnating with UF Resin J. Han, K.N. Liu and X.T. Gao	54
Effect on the Microstructure and Properties of WC-10% Co Alloy Co-Doped with NbC and Cr₃C₂ H. Yu, W.N. Li, X.Q. Jiang and P.H. Jiao	58
Preparation of Sludge Activated Carbon Adsorbent and its Engineering Simulation Study to Removing Odor W. Jiang, Z.L. Gong, L.H. Zhang, B. Yan and A.X. Jiang	62
A Generalized Route to Synthesize Nanometer-Sized Metal Oxides by Using Frothing Method Z.L. Cheng and Z. Liu	66
Citric Based Sol-Gel Synthesis and Photoluminescence Properties of Eu³⁺ Doped NaSrBO₃ Phosphors X.J. Wang, H.L. Li and Z. Sun	70
Effect of Heat Treatment to Ni-20wt.%Al Coating Diffusion J.X. Wang, J.F. Sun and Z.P. Wang	75
Study on Synthetic Process of Low Toxic Urea-Formaldehyde Resin G.H. Chen, J. Han and X.H. Zhang	79
Characterization of Antibacterial Effects of Novel Silver Nanoparticles: A Case Study on <i>Pseudomonas</i> as a Model for Gram-Negative Bacteria T.T. He, Y.Z. Zhou, J. Yang and H.F. Shi	83

Effects of Hydrothermal Treatment on the Structure and Properties of Aviation Polysulfide Sealant	
J.Y. Meng and Y.Y. Wang	87
Protein Adsorption on Surface-Attached Weak Polyelectrolyte Layers	
Q. Li and H.N. Zhang	93
Research and Evaluation on the Machining Properties of Plantation <i>Eucalyptus</i> Veneer LVL	
J. Sun, N. Li, C.W. Su, Q.P. Yuan and W.J. Fang	97
Preparation of Conductive Adhesives by Ag/CNTs Composite Nano-Particles	
Y.C. Feng and X.X. Zheng	103
Gold Nanoparticles Self-Assembling on Surfaces of Carbon Nanotubes Modified by Mercapto Groups	
Y.C. Feng and G.L. Zhou	107
Study of Preparation and the Influencing Factors of Chrysanthemum-Shaped Calcium Carbonate Applied to Paper Industry	
Z.L. Chen and H.J. Zhu	111
Preparation and Corrosion Behaviour of Micro-Arc Oxidation Coating on Ti6Al4V Alloy	
X.Z. Lin, M. Gong, Z.H. Wang and P. Zhang	117
Phloridzin Isolated from Apple Pomace by Resin	
D. Liu, H. Shang and H.J. Ji	121
The Mineral Chemistry and Classification of New Ordinary Chondrites Collected in Antarctica	
B.H. Wang, S.J. Li and B.K. Miao	125
Preparation and Characterization of Cyclophosphamide-Loaded Chitosan Microspheres	
Y.L. Ding, S.S. Ding and G.F. Ding	130
Study on Adsorption Properties of Anion Exchange Fiber	
S. Yang and W. Zheng	134
PPS/Metal Composite Materials Preparation and Friction Performance	
Z.G. Luo, B. Zhao, J. Li and J.W. Xu	139
Research on the Control of ZnO Nanostructures Morphology via a Reverse Micellar Route	
R. Li and Y.T. Wang	143
Discuss the Applications of the Automotive Lightweight Materials in China Briefly	
X.J. Wang and Y.S. Chen	148
Control on the Photoluminescence of ZnO Nanostructures Synthesized by a Reverse Micellar Route	
Y.T. Wang and R. Li	153
Synthesis of Microcrystalline Cellulose Grafting Poly (methyl methacrylate) Copolymers by ATRP in 1-Allyl-3-Methylimidazolium Chloride	
E.J. Tang, M. Yuan, L. Li, F. Bian and D.S. Zhao	157
Observation of a Lamella Structure in a Baked Carbon	
K.Y. Wen, Y.L. Xu, L.L. Li, J.M. Chen and P. Xiao	162
High Thermoelectric Performance of p-Type Bi_{0.5}Sb_{1.5}Te_{3+x}Te Crystals Prepared via Gradient Freezing	
T.H. Liang, S.Q. Yang, Z. Chen and Q.X. Yang	167
Photoreactive Carbon and Nitrogen-Codoped ZnWO₄ Nanoparticles: Synthesis and Reactivity	
S.H. Chen, B.X. Wang, X.H. Qiu and Z.S. Xiong	172
Surface Micro-Structure Effect the Combustion and Mechanical Properties of Triple Base Propellants	
F.Y. Zhang, P. Du and X. Liao	178
Cytotoxic Effects of Transforming Growth Factor-α Conjugated with Cytotoxin Saporin on Proliferating Vascular Smooth Muscle Cells	
J. Yang, C. Chu, B. Deng, S.L. Ding, G.H. Wang, Y. Zhang and Z.H. Quan	182

Chapter 2: Advanced Manufacturing Technology

Computational Fluid Dynamics Analysis of Working Fluid Flow and Machining Debris Movement in End Electrical Discharge Milling and Mechanical Grinding Compound Machining	
R.J. Ji, Y.H. Liu, C. Zheng, F. Wang, Y.Z. Zhang, Y. Shen and B.P. Cai	191
Research on CFD Simulation of the Cement Slurry Mixer	
S.P. LI, Y.L. Yuan and L.G. Shi	196
Wind Power Prediction Based on Similar Day Clustering Support Vector Machine	
X.B. Wang, Z.Y. Ding, P. Yang and X. Yang	200
Study on Turbine Blade Abrasion Mechanism and Abrasion Resistance Performance Testing Machine	
H.P. Li, F. Li, Z.F. Fang and Y.Q. Chen	206
Study on Cutting Process of Manual Thermite Cutting Technology	
S. Wang, W.T. Xin, L.F. Qu and Y.Y. Wu	211
Research on Contact Force Control in Process of Aspheric Surface Polish	
J.Q. Lin, T.H. Ran and L. Feng	216
Research on Exhaust Gas Temperature inside Catalytic Honeycomb Monolith Channel of Natural Gas Burner Start-up	
Z.H. Wang and S.H. Zhang	223
The Stress Change Simulation Analysis for Beam Blank Cogging during H-Beam Rolling	
L. Chen, Z.Y. Li and K.X. Bi	228
A New Experimental Identification Method for Fluid-Induced Force in Labyrinth Seals	
D. Sun, Y.T. Ai, W.F. Zhang and J.G. Yang	232
Multi-Fields Coupled Simulation on Casting Process of Aluminum Alloy Based on Heat Conduction by Rotating Heat Pipe Bundle	
J.M. Chen, Y.Q. Li and J.Q. E	237
Experimentation and Research of Three-Phase Switching Synchronous Operation of Novel High Speed Switch Gear	
E.Y. Dong, J.H. Zhao, Y.H. Bi, Y.X. Wang and X.Y. Duan	246
The Study on the Reliability of the Collection System of the Offshore Wind Farms Considering the Electrical Faults and Switchgear Configurations	
R.S. Tan, P. Yang and P. He	250

Chapter 3: Sustainable Manufacturing Technologies

Optimization of the Submerged Fermentation Conditions of Ganoderma Lucidum with High Triterpenoids Production by Response Surface Analysis	
M.L. Cui and G.Q. He	259
The Rule of Migration and Transformation of Naphthalene in Groundwater	
Z.J. Liu, M. Hong and D.L. Zhang	263
A Pseudo-Fourier Series Method and its Application in Tilt Data Processing	
Y. Wu, S. Yang and X.Y. Zhao	268
The Efficiency of Material Utilization and Energy Conversion of Biogas Fermentation by Annua	
C.M. Wang, W.D. Zhang, Y.B. Chen, F. Yin, S.Q. Liu, X.L. Zhao and J. Liu	273
Evaluation of an Aerobic Denitrifying Bacterium for Wastewater Treatment	
D.Y. Zhang, X.Y. Shen, X.L. Xu, Y. Lu and F.L. Hao	278
Algae-Removal Treatment of A-F/PDM Composite Coagulants to Summer Taihu Lake Algae-Rich Water under Prechlorination Process	
X.L. Zhao, Y.J. Zhang, X.X. Li and C. Liu	283
The Integrated Evaluation Research on the Reverse Logistics of End-of-Life Vehicle Based on Green Manufacturing	
N. Yu, Y.P. Yang, R.S. Yin and D.D. Guo	287
Tendency of Beach Surface between Maojiagang Two Moles	
K.D. Wang and J.H. Wang	292
Phosphate Removal from Aqueous Solution Using Fly Ash Modified with Magnetic Fe-Zn Bimetal Oxide	
K. Xu, T. Deng, C.G. Li and J.L. Niu	296

Research on a Novel Environment-Friendly Synthetic Material Based on Sludge Z.H. Xu, D.F. Zhang, L.L. Wu and S.H. Li	303
--------------------------------------------------------------------------------------------------------------------------------	-----

Chapter 4: Advanced Design Technology

Digital Walking Control System Study for Asphalt Paver Based on DSP W. Tao	309
Design of Automatic Nucleic Acid Extraction Instrument Based on Magnetic Nanobeads Y.J. Dou, J.S. Xu, C.L. Deng, X.L. Zhao, L. Nie, Y. Yu, M. Wang and T. Song	313
Design and Engineering Verification of HTR-PM Fuel Handling H.Q. Zhang, X. Wang, H.K. Li, J.F. Nie and J.G. Liu	317
Design of a New Kind of the Radial Annular Seal for the Aeroengine D. Sun, Y.T. Ai, W.F. Zhang and J.G. Yang	326
Collaborative Design of the Injection Mould C.H. Liu	330
An Improved MPPT Algorithm for Off-Grid Wind Power Generator Based on Hill Climbing Method P. Yang and P.S. Liang	334
Line Loss Rate Forecasting Based on Grey Model and Combination of Neural Network F. Xie, B.X. Zhou, Q. Zhang and L. Jiang	340
The Classification Research about the Uncertain Factors of Job Shop Manufacturing Shop Re-Scheduling M.G. Ge, M.Z. Liu, M.X. Zhang, J. Hu, W.R. Wu and L. Ling	344
An Embedded Positioning System Applied to the Seismic Exploration B. Zhang, L.L. Xing, D.Q. Chen, L. Xie, Y. Li and Q.B. Ouyang	348
A Simulation Model for Multi-Factor Sensitivity Analysis on Energy Demand Z.F. Tan, S.X. Wang, C. Zhang, L.Q. Lin and Y.H. Zhao	352
An Improved Particle Swarm Optimization Algorithm with Invasive Weed H. Zhao, J.L. Yu, A. Tahmasebi and P.H. Wang	356
Monitoring of Efficiency and NO_x Emissions at a Coal-Fired Utility Boiler H. Zhao, J.L. Yu, A. Tahmasebi and P.H. Wang	360
Color Image Segmentation Based on Dynamic Model and Power Spectrum Y.P. Chen, Y.H. Qiao and J. Miao	364
Study on Integrated Project Delivery Construction Project Collaborative Application Based on Building Information Model J.Y. Teng, X.G. Wu, G.Q. Zhou, W.J. Zhao and J. Cao	370
Study on Electronic Kanban Management System in Steel Structure Engineering of an International Expo Centre J.L. Guo, J.Y. Teng, S.Q. Li, D.Y. Wan and X. Jiang	375

CHAPTER 1:

New Materials and Advanced Materials

Investigation on nano-sized ZnO powder doped with Al³⁺ prepared by sol-gel method

Xiong Yu^{1,a}, Zheng Ji^{2b}, Li Songlin^{2c}, Liu Xuejia^{1d}, Liang Lu^{1e}

¹. Beijing Institute of Aeronautical Materials, Beijing 100095, China

². School of Materials Science and Engineering, Tianjin University, Tianjin 300072, China

^a xyubiam@sina.com ^b zheng_ji@tju.edu.cn ^c slli@tju.edu.cn

Keywords: Sol-gel process; ZnO₂; Al³⁺-doped; Electric conductivity

Abstract. Al³⁺-doped ZnO nano-powder was prepared by sol-gel process, using tin tetrachloride and titanium tetrachloride as starting materials. The crystallinity and purity of the powder were analyzed by X-ray diffraction spectrometer (XRD). And the size and distribution of Al³⁺-doped ZnO grains were studied using transmission electron microscope (TEM) and scanning electron microscope (SEM). The results showed that the Al³⁺ was successfully doped into the crystal lattice of tin oxide and that the electric conductivity of Al³⁺-doped ZnO sample was improved significantly.

1. Introduction

ZnO doped systems have attracted a lot of attention all over the world due to their good conductivity, high whiteness, environmentally friendly behavior and non-toxic property. These ZnO materials are mainly used as antistatic agent and have significance in research and application, and their market demand is growing rapidly. [1,2] The number of conduction electrons increase according to the doping content of Al or Ga [3,4]. The substitution of doping ions for zinc ions weakens the electron binding capacity of ionic bond. The number of free electrons activated from valence electrons increase, which make excess electrons show up in the bottom of conduction band, and the carrier concentration of the internal crystal increase accordingly. Moreover, oxygen vacancies are generated in the doping process. With the increase of doping content, number of free electrons and carrier density, the conductivity of powder decreases [5-9].

In this work, the authors prepared Al³⁺-doped ZnO using sol-gel technique and investigated the microstructure, size, distribution and crystallization of Al³⁺-doped tin oxide grains as well as the doping effects on the electrical conductivity of these materials.

2. Experimental

The ZnO gel was prepared by sol-gel technique. A brief description was given in the following. Tin tetrachloride, (Zn(NO₃)₂·6H₂O) was first resolved into the solution composed of ethanol and de-ionized water (volume ratio is 1:1) to a concentration of 2 mol/l with vigorous stirring for a few minutes, and then adding titanium tetrachloride (Al(NO₃)₃·9H₂O) to the solution with the dispersant of polyethylene glycol (PEG) and stirring for 30 minutes at 80°C. Ammonia was added to the solution until the pH of the mixture reached 7. ZnO gel was rinsed by de-ionized water and ethanol after 48 hours of aging until there was no chloride ion. Then the gel was dried in an oven at 60°C for 4 hours, and then respectively sintered for 2 hours at 300°C, 500°C and 700°C to get different Al³⁺-doped ZnO powders.

The morphologies of Al³⁺-doped ZnO powders were observed by scanning electron microscopy (SEM; PHILIPS XL-30 TMP ESEM). And its XRD patterns were obtained using Rigaku Dmax X-ray diffractometer with a copper Ka X-ray source, 40 kV and 100 mA.

3. Results and Discussion

3.1 TEM

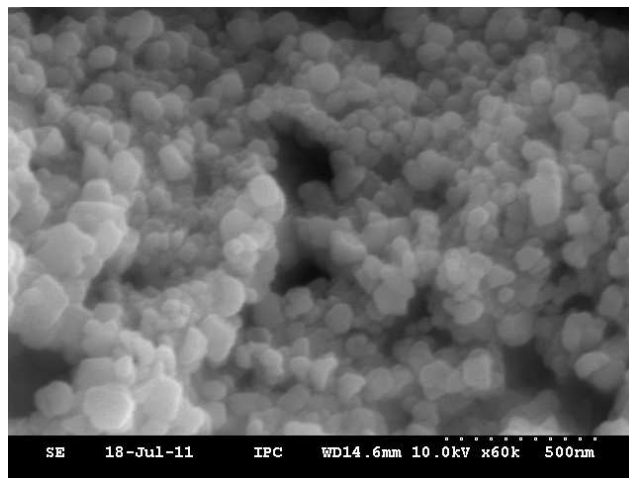


Fig.1. SEM image of Al^{3+} -doped tin oxide gel grains

The microstructure and distribution of Al^{3+} -doped ZnO gel grains were shown in Fig.1. It was found that the grains varied in size from 10 to 100 nm and evenly distributed during the formation of gel, which revealed that polyethylene glycol (PEG) could effectively prevent ZnO gel grains from agglomerating. These phenomena should be ascribed to the repulsive force among the gel grains and the electric double layer of gel, generated by the organic polymerization chain reaction of PEG in the solution.

3.2 XRD

Fig.2 showed the XRD spectra of Al^{3+} -doped ZnO powders sintered for 2 hours at 350°C, 500°C and 700°C, respectively. The measurements demonstrated that there existed only the peaks of ZnO while the peaks of Al^{3+} didn't occur in all XRD spectra, which revealed that the Al^{3+} was successfully doped into the crystal lattice of ZnO by sol-gel technique. As shown in Fig.2, the intensity of ZnO peaks increased with the increase of sintering temperature and the half-height width of peaks decreased with the increase of temperature, which indicated that the crystallization of ZnO powder developed progressively as the sintering temperature increased. In this work, the crystallization of ZnO gel sintered at 350°C didn't grow thoroughly while perfect crystal of ZnO could be obtained at higher sintering temperature, such as 500°C and 700°C. The grain size of Al^{3+} -doped ZnO powders sintered at different temperatures could be calculated according to the Scherrer. The results were shown in Table 1.

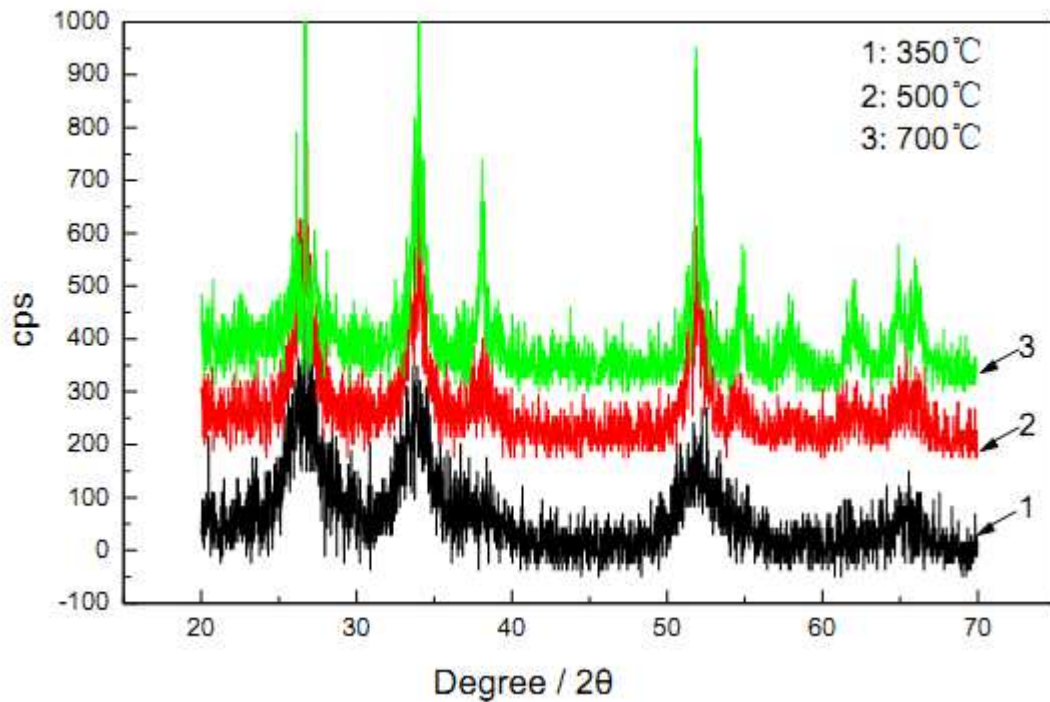


Fig.2. XRD spectra of the Al^{3+} -doped ZnO powders sintered for 2 hours at 350°C, 500°C and 700°C, respectively.

Table 1 Grain size of Al^{3+} -doped SnO_2 powders sintered at different temperature

Temperature (°C)	350	500	700
Grain size (nm)	10-20	30-50	70-90

It could be concluded that the Al^{3+} -doped ZnO powders sintered at 500°C was more suitable for further study because the grains aggregated easily at 700°C, which were also supported by SEM images (shown in Fig.3).

3.3 SEM

Fig.3 showed the microstructure of Al^{3+} -doped ZnO_2 powders sintered for 2 hours at 500°C and 700°C, respectively. It could be observed that grain size of ZnO powders sintered at 700°C were much larger than that of powders sintered at 500°C. As shown in Fig.3, the grains of powders sintered at 500°C distributed evenly while those of powders sintered at 700°C agglomerated, which indicated that hard agglomeration of doped tin oxide powder occurred at higher temperature, e.g. 700°C in this work.

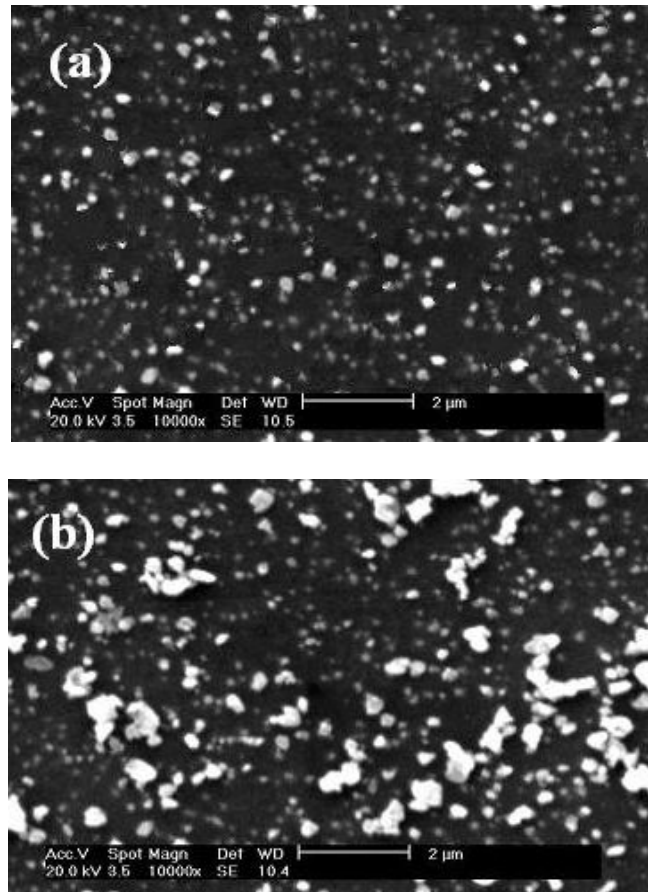


Fig.3. SEM images of Al^{3+} -doped ZnO powders with sintered at different temperatures for 2hours, respectively. (a)500°C, (b)700°C

3.4 Analysis of physical properties

As shown in Table 2, the density of Al^{3+} -doped ZnO powders was higher than that of pure ZnO prepared by the same method. And the electric resistivity of Al^{3+} -doped ZnO materials was 10^4 times higher than that of pure ZnO materials. It could be concluded that Al^{3+} doped into the lattice of ZnO intensively enhanced the electric resistivity of these materials, which was due to the following reasons.

Table 2. The density and electric conductivity of ZnO materials

Materials	Electric resistivity ($\Omega \cdot \text{cm}$)
Pure ZnO	5.23×10^8
Al^{3+} -doped ZnO	3.142×10^4

4. Conclusions

From the test results discussed above, it could be inferred that it was possible to make nano-sized Al^{3+} -doped ZnO using sol-gel technique. Polyethylene glycol (PEG) could effectively prevent ZnO gel grains from agglomerating during the formation of the gel. It was achievable to get perfect Al^{3+} -doped ZnO crystal and fine grains when dried Al^{3+} -doped ZnO gel was sintered at 500°C. The testing results revealed that the doped Al^{3+} could significantly enhance the electric conductivity of ZnO materials as well as the density.

References

- [1] Lambrecht, W. R. L., A. V. Rodina, et al. Valence-band ordering and magneto-optic exciton fine structure in ZnO. *Physical Review B*, 2002, 65(7): 1-12
- [2] Meyer, B. K., H. Alves, et al. Bound exciton and donor-acceptor pair recombinations in ZnO. *Physica Status Solidi B-Basic Research*, 2004, 241(2): 231-260
- [3] Janotti, A. and C. G. Van de Walle . Native point defects in ZnO. *Physical Review B*, 2007, 76(16): 1-22
- [4] Meyer, B. K., J. Sann, et al. Incorporation of acceptors in ZnO. *Advances in Solid State Physics* 45. B. Kramerr, 2005, 45: 289-299
- [5] Meyer, B. K., J. Sann, et al. Shallow donors and acceptors in ZnO. *Semiconductor Science and Technology*, 2005, 20(4): S62-S66
- [6] Look, D. C., G. C. Farlow, et al. Evidence for native-defect donors in n-type ZnO. *Physical Review Letters*, 2005, 95(22): 340-342
- [7] Liu, Y., J. Zhou, et al. Preparation and characterization of nano-zinc oxide. *Journal of Materials Processing Technology*, 2007, 189(1-3): 379-383
- [8] Cox, S. F. J., E. A. Davis, et al. Experimental confirmation of the predicted shallow donor hydrogen state in zinc oxide. *Physical Review Letters*, 2011, 86(12): 2601-2604
- [9] Takaki, T., K. Kurosawa, et al. Electrolytic Synthesis of Al-Doped ZnO Nanopowders With Low Electrical Resistivity. *Journal of the American Ceramic Society*, 2010, 93(10): 3088-3091

Mechanical Properties of Recycled Butyl Rubber/Virgin Butyl Rubber Composite

Lin Li^{1,a}, Jin Kuk Kim^{1*,b}

¹School of Nano & Advanced Materials Engineering, Gyeongsang National University, Gyeongnam, Jinju, 660-701, South Korea

^aqustlilin@hotmail.com

^b rubber@gnu.ac.kr

Keywords: Recycled rubber, composite, mechanical properties

Abstract:

Large amounts of butyl rubber (IIR) are used as inner tires for aeroplanes, trucks, cars, two-wheelers etc. However, after long runs when these tires are not serviceable they are discarded. Almost the entire amount of rubber from the worn out tires is discarded, which again need very long time for natural degradation due to crosslinked structure of rubbers and presence of additives. To solve this problem, recycled rubber is used as a partial substitute for new IIR in inner tire compounds. The blends with a certain amount of recycled rubber content show good mechanical properties.

Introduction

Thermosetting materials like rubbers on processing and molding are crosslinked, and therefore cannot be softened or molded by heating again. The technology for recycled of thermoset polymers including rubbers is complex, costly and less viable commercially. [1] Recently the use of reclaimed/reground thermoset resins in new polymer formulations is found to have some influence on flow and deformation characteristics during processing. [2-4]

Experimental

Materials

The rubbers, recycled IIR and new IIR, along with CB (N660), N-cyclohexyl-2-benzothiazolsulfenamide (CBS), zinc oxide, stearic acid, CaCO₃, processing oil (A#2), and sulfur were all supplied by NEXEN Tire Co. Ltd., Korea.

Sample preparation

Mixing was performed in a 200 ml Banbury mixer at a rotor speed of 60 rpm for the mixing stage at a temperature of 120°C. The recycled IIR/new IIR blends at the desired ratio were loaded into the mixer and premixed for 2 min. Then, the zinc oxide (5 phr), stearic acid (1 phr), CaCO₃ (10 phr) and CBS (2.5 phr) were added and mixed for 4 min. Next, half of the required amount of CB was added and compounded into the rubber for 1.0 min followed by the other half of the CB, mixed for 2.5 min and then the mixture was discharged onto the roll mill at 80°C, where the sulfur (1.5 phr) was added.

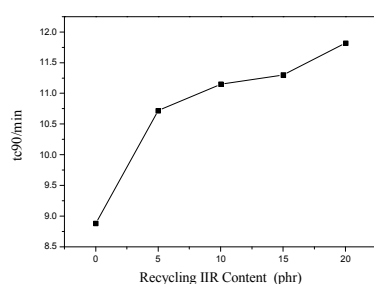
The cure behavior of the compounds was determined at 165°C using a Monsanto Oscillating Disc Rheometer (Model ODR 2000, Monsanto, St. Louis, MO) at 1° arc (ASTM D208488).

Results and discussion

The compound formulation is given in Table 1. All blends have the same chemical composition, exception for the ratio of recycled IIR to virgin IIR.

Table 1 Formulations of recycled IIR and virgin IIR blends

Ingredient	1#(phr)	2#(phr)	3#(phr)	4#(phr)	5#(phr)
Recycled IIR/ New IIR	0/ 100	5/95	10/90	15/85	20/80
Carbon Black	55	55	55	55	55
Oil (A#2)	5	5	5	5	5
Zinc oxide	5	5	5	5	5
Stearic acid	1.0	1.0	1.0	1.0	1.0
Sulfur	1.5	1.5	1.5	1.5	1.5
CBS	2.5	2.5	2.5	2.5	2.5
CaCO ₃	10	10	10	10	10

Fig. 1 T_{c90} of blends as a function of recycled rubber content

The optimum cure time(Tc90) is the vulcanization time required to obtain the optimum physical properties. It can be observed in Fig. 1 that the optimum cure time varies drastically with increasement of recycled IIR.

It is evident that the compounds acquire higher optimum cure time with increase in the amount of recycled IIR. It is possible that the recycled rubber with a cross-linked network hinders the mobility of the unsaturated segments of virgin IIR, thus accounting for the lower cure rates. And the apparent reason for the Tc90 increase is that cross-linked recycled IIR does not easily flow to the matrix, so the increase in recycled IIR loading may reduce the flow and consequently increase the torque. It is also believed that the highly aggregated and convoluted structure of waste rubber powder contains void space in which the matrix rubber is trapped, which increases the effective volume fraction of waste rubber and results in higher viscosity of the blends.

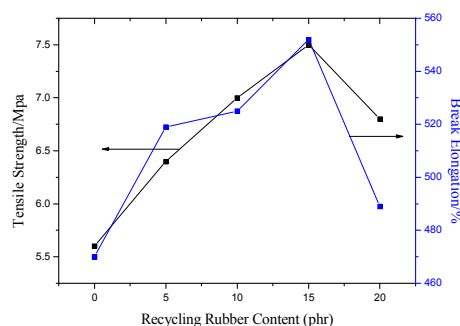


Fig. 2 Tensile strength and break elongation of blends as a function of recycled rubber loading in virgin IIR matrix

Tensile strength and elongation at break are used to evaluate the mechanical properties of the systems in figure 2. The recycled IIR and virgin IIR compounds have much better properties. It is worth noting that with up to 15 phr loading of recycled IIR, the compound has even higher tensile strength and elongation. As could be expected, better compatibility and the migration of sulphur between the recycled IIR and virgin IIR matrix are achieved and better properties are obtained. However, with up to 15 phr loading of recycled IIR, tensile strength falls significantly. It is also found that elongation at break decrease with higher content of recycled IIR.

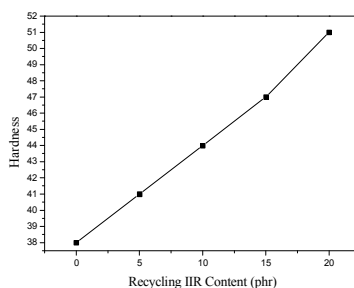


Fig. 3 Hardness of blends as a function of recycled rubber content

Fig. 3 shows that an important increase in hardness with recycled IIR loading is observed because recycled IIR is probably harder than virgin IIR after devulcanization.

Summary

Waste IIR of 5, 10, 15 and 20 phr is added to a virgin rubber matrix in the form of recycled IIR. With increase in the proportion of recycled IIR, the optimum cure time is extended. It is found that the addition of recycled rubber with an adequate amount produces the better mechanical performance. So it is possible to maintain good mechanical properties of the compounds of virgin IIR/ recycled IIR and lower the cost at the same time.

Reference

- [1] Throne JL, Effect of recycle on properties and profits: Algorithms, Adv. Polym. Technol. 7 (1987) 347-360.
- [2] C. Jacob, P.P. De, A.K. Bhowmick, S.K. De, Recycling of EPDM waste. I. Effect of ground EPDM vulcanizate on properties of EPDM rubber, J. Appl. Polym.Sci. 82 (2001) 3293-3303.
- [3] C. Jacob, A.K. Bhattacharya, A.K. Bhowmick, P.P. De, S.K. De, Recycling of ethylene propylene diene monomer (EPDM) waste. III. Processability of EPDM rubber compound containing ground EPDM vulcanizates, J. Appl. Polym. Sci. 87 (2003) 2204-2215.
- [4] H. Ismail, R. Nordin, A.M. Noor, Cure Characteristics, Tensile Properties and Swelling Behaviour of Recycled Rubber Powder-Filled Natural Rubber Compounds, Polym. Test. 21 (2002) 565-569.

Synthesis and characterization of acrylamide based benzoxazine

Bakangura Erigene^a, Luo Zhongyu, Wang Guangkai, Yang Bin, Yue Yanping,
and Lin Xiaodan^b

College of Materials Sci. and Eng., South China Univ. of Tech., Guangzhou 510640, PR China

^abaka.eri@hotmail.com, ^bmcsxdlin@scut.edu.cn

Keywords: benzoxazine, acrylamide-benzoxazine, ring opening curing, thermal polymerization, solvent effect

Abstract. Novel benzoxazine monomers, acrylamide based benzoxazine, have been prepared from direct condensation of phenols with acrylamide and formaldehyde. ¹H NMR and FT-IR, DSC and TGA were used to analysis the structure, compositions and investigate the curing behaviour and thermal stability, respectively. Solvent effects were studied. Solventless method is good for higher formation ratio of benzoxazine to the corresponding phenolic resin. The ratio for P-AA is 36.4% by solventless method, while it's about 26% by toluene solvent; and 44% and 20% for B-AA, respectively. The monomers mixtures exhibit curing temperature (ca.187°C) without catalysts lower than their related allyl-benzoxazine. The FT-IR of different curing temperature shows the disappearance of double bond absorption at 1668 cm⁻¹ and oxazine ring at 1232 cm⁻¹ and appearance of hydroxyl group at 3446 cm⁻¹. Thermal stability of cured benzoxazine show good char residues compared with traditional benzoxazine of aniline.

Introduction

Polybenzoxazines are phenolic resins which have wide application in aerospace, constructions, automobiles, electronic devices, adhesives and coatings^[1]. Polybenzoxazine, contrary to traditional phenolic resins, possess excellent characteristics such as non volatile upon curing, low volumetric change, catalyst and halogen free. Polybenzoxazines suffer brittleness, low process ability and require high curing temperature. Different strategies taken to design suitable benzoxazine include preparation of monomers with addition functional group, blending, incorporation of benzoxazine structure to other polymers and hybridization with inorganic materials. From the first methodology, benzoxazine with various amines^[2a], naphthols^[2b], acetylene^[2c], propargyl ether^[2d], maleimide and norbornene^[2e], epoxy^[2f], allyl^[2f,2g,2h] caumarin^[2i], and urethane^[2j] were reported.

Mostly, benzoxazine monomers have been synthesized by condensation of primary amines, phenols and formaldehyde. Aversa et al^[3] synthesized benzoxazines with other route such as Mannich reaction between 2, 4-dimethylphenol, formaldehyde solution and 3-aminopropanoic acid in ethanol, direct ortho-lithiation of phenol^[4], direct ortho-metalation^[5], and the reactions of salicylamines (o-hydroxybenzylamine) with glyoxal or diketones in methanol^[6], respectively. Ishida et al, have extensively studied the mechanism of reactions of condensation of primary amines, phenol and formaldehyde in both solution and solventless method^[7-10].

Acrylamide and its polymer, polyacrylamide, have vast application in various fields such as water treatment, paper milling and minerals processing, testing and engineering^[11]. Interestingly, amide groups may improve stiffness and adhesion of incorporating polymers. Heretofore, no benzoxazine was synthesized from direct Mannich reaction of amides. Acrylamide^[12-14] can undergo